Functional Properties of the Heme Propionates in Cytochrome *c* Oxidase from *Paracoccus denitrificans.* Evidence from FTIR Difference Spectroscopy and Site-Directed Mutagenesis[†]

Julia Behr,[‡] Hartmut Michel,[‡] Werner Mäntele,[§] and Petra Hellwig*[,§]

Max-Planck-Institut für Biophysik, Abteilung Molekulare Membranbiologie, Heinrich-Hoffmann-Strasse 7, D-60528 Frankfurt/M., Germany, and Institut für Biophysik, Theodor-Stern-Kai 7, Haus 74, D-60590 Frankfurt/M., Germany

Received June 30, 1999; Revised Manuscript Received November 10, 1999

ABSTRACT: By specific ^{13}C labeling of the heme propionates, four bands in the reduced-minus-oxidized FTIR difference spectrum of cytochrome *c* oxidase from *Paracoccus denitrificans* have been assigned to the heme propionates [Behr, J., Hellwig, P., Mäntele, W., and Michel, H. (1998) *Biochemistry 37*, 7400−7406]. To attribute these signals to the individual propionates, we have constructed seven cytochrome *c* oxidase variants using site-directed mutagenesis of subunit I. The mutant enzymes W87Y, W87F, W164F, H403A, Y406F, R473K, and R474K were characterized by measurement of enzymatic turnover, proton pumping activity, and Vis and FTIR spectroscopy. Whereas the mutant enzymes W164F and Y406F were found to be structurally altered, the other cytochrome *c* oxidase variants were suitable for band assignment in the infrared. Reduced-minus-oxidized FTIR difference spectra of the mutant enzymes were used to identify the ring D propionate of heme *a* as a likely proton acceptor upon reduction of cytochrome *c* oxidase. The ring D propionate of heme a_3 might undergo conformational changes or, less likely, act as a proton donor.

Cytochrome *c* oxidase is the terminal enzyme of the respiratory chain in mitochondria and many bacteria. It catalyzes electron transfer from cytochrome *c* to molecular oxygen, thus reducing the latter to water. In the course of this reaction, four protons are pumped from the cytoplasmic to the periplasmic side of the membrane (in prokaryotes) or from the matrix to the intermembrane space (in eukaryotes). The protons consumed by water formation are taken up from the cytoplasmic/matrix side, whereas cytochrome *c* donates its electron from the opposite side of the membrane. Altogether eight charges are translocated across the membrane. The resulting proton and charge gradient drives ATP synthesis by the ATP-synthase. In cytochrome *c* oxidases, the first electron acceptor is a binuclear Cu_A center close to the outer surface. From there the electron is transferred to a heme *a*, and then to a heme a_3 and Cu_B binuclear site, where oxygen binding and reduction takes place. These latter three electron acceptors are imbedded into the hydrophobic part of the membrane. Based on the X-ray crystallographic structural analysis of the *Paracoccus denitrificans* cytochrome *c* oxidase (*1, 2*) and the results of site-directed mutagenesis, two potential proton-transfer pathways have been identified (*3, 4*). In the so-called K-pathway, protons might be transferred from S291 to the crucial residue K354, then to T351 and to the hydroxy group of the hydroxyethylfarnesyl side chain of heme a_3 and further to Y280, which appears to be covalently cross-linked to the Cu_B ligand H276 (*2, 5*). The presence of K354 seems to be essential for the reduction of heme a_3 (*6*). It is still under debate whether the K-pathway is also used in the latter parts of the catalytic cycle (*7*). In models of the catalytic cycles of cytochrome *c* oxidases, the latter parts comprise the transition of the R-state (where Cu_B and heme a_3 are reduced) to a P-state (where oxygen has been bound and converted to a "peroxy" intermediate), then to an oxoferryl state (F-state) after the third electron transfer, and back to the oxidized form (O-state) after the fourth electron transfer. It has been postulated that the P→F and F→O transitions are coupled to proton pumping, with consumption of two protons, formation of one water molecule, and two protons pumped per transition (*8*). However, this view has been challenged recently (*9*).

The second potential pathway, the D-pathway, leads from D124 via several polar residues and a presumably water-filled cavity to E278. The protons might be transferred directly to the binuclear site via a temporarily established chain of water molecules. The protons could also be translocated to the ring D propionate of heme a_3. Both residues could approach one another to hydrogen bonding distance by conformational changes (*1*). Alternatively, water molecules might be involved in the proton transfer to the heme a_3 propionate. The D-pathway has been suggested to be essential for the steps from the P- to the O-state (*10, 11*).

Proton uptake measurements showed that about 2.5 protons are taken up upon full reduction of cytochrome *c* oxidase, about 0.5 of which appears to be associated with Cu_A/heme *a* reduction and the remaining 2 with the binuclear center (*12, 13*). As a motor for coupling oxygen reduction and proton pumping, a principle of charge compensation has been

[†] Financial support from DFG (Ma 1054/17-1 and 17-2 to W.M.) is gratefully acknowledged.

* To whom correspondence should be addressed. Email: hellwig@biophysik.uni-frankfurt.de. Telephone: 49-69-6301-5835. Fax: 49-69-6301-5838.

[‡] Max-Planck-Institut für Biophysik.

[§] Institut für Biophysik.

10.1021/bi991504g CCC: $19.00
Published on Web 01/20/2000

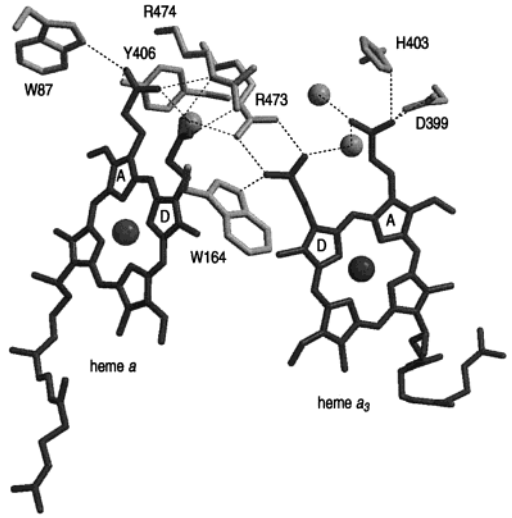

FIGURE 1: Potential hydrogen bonds between the four heme propionates and surrounding amino acid side chains and three water molecules.

postulated (*14*). The reduction of the binuclear center might cause the uptake of protons from the cytoplasm, which are later expelled into the periplasm by the protons consumed in water formation. The same principle could apply to the redox changes of heme *a* (*9*). Interestingly, E278 is 12.3 Å away from the heme a_3 Fe atom and 12.8 Å away from the heme *a* Fe atom, so that reduction of either heme a_3 or heme *a* might drive proton uptake through the D-pathway (*9*). The heme propionates are possible candidates for being protonated upon reduction of the binuclear center or/and heme *a*.

In a previous study we demonstrated redox-dependent changes of at least two of the four heme propionates in cytochrome *c* oxidase from *Paracoccus denitrificans* by specific ^{13}C labeling and FTIR spectroscopy (*15*). In the reduced-minus-oxidized FTIR difference spectrum, a negative signal at 1570 cm^{-1} and a positive signal in the 1546−1528 cm^{-1} range have been assigned to antisymmetric COO^- modes of deprotonated heme propionates. A negative signal at 1676 cm^{-1} has been assigned to a COOH mode of a protonated heme propionate and the negative signal at 1390 cm^{-1} to a symmetric COO^- mode of a heme propionate (*15*).

As revealed by the X-ray structure analysis of cytochrome *c* oxidase from *Paracoccus denitrificans* (*1, 2*), the four heme propionates are in hydrogen bonding distances to the amino acid side chains of W87, W164, D399, H403, Y406, R473, and R474 and to three water molecules (Figure 1). In Table 1 the donor−acceptor distances of the potentially formed hydrogen bonds are given; in addition, the two potential hydrogen bonds to the protein backbone are listed. To modify the local environment of the heme propionates and to assign the heme propionate signals in the redox-induced FTIR difference spectrum to specific heme propionates, these amino acid residues were exchanged by site-directed mutagenesis with the exception of D399. Mutagenesis of D399 has already been reported by Pfitzner et al. (*16*), and electrochemically induced FT-IR difference spectra are described in ref *17*.

Table 1: Lengths of the Potential Hydrogen Bonds, As Revealed by X-ray Crystallography of *the P. denitrificans* Cytochrome *c* Oxidase (*2*) between the Heme Propionates and Surrounding Groups[a]

heme propionate	amino acid residue/ water molecule	distance (Å)
ring A propionate of heme *a* (O1)	W87 (Nϵ1)	3.3
	Y406 (OH)	3.1
ring A propionate of heme *a* (O2)	R474 (N)	2.6
	H_2O	2.6
ring D propionate of heme *a* (O1)	W164 (N)	3.1
	R474 (NH2)	2.7
ring D propionate of heme *a* (O2)	R473 (NH2)	3.5
	R474 (Nϵ)	2.9
	H_2O	2.8
ring A propionate of heme a_3 (O1)	D399 (Oδ1)	3.1
	D399 (Oδ2)	2.7
	H403 (Nδ1)	2.9
ring A propionate of heme a_3 (O2)	H_2O	3.1
	H_2O	2.7
ring D propionate of heme a_3 (O1)	W164 (Nϵ1)	3.0
	R473 (NH2)	2.9
ring D propionate of heme a_3 (O2)	R473 (NH1)	3.1
	H_2O	3.1

[a] The interactions listed also comply with the geometry for hydrogen bond formation.

EXPERIMENTAL PROCEDURES

Paracoccus denitrificans was grown aerobically in succinate medium (*18*) at 32 °C and harvested at late exponential phase. Membranes were prepared as described (*19*). After solubilization with the detergent *n*-dodecyl-β-D-maltoside, the protein was purified by streptavidin affinity chromatography (*20*). For affinity purification of a cytochrome *c* oxidase−F_v complex, an engineered monoclonal antibody fragment (F_v) linked to a strep tag and directed against an epitope on the periplasmic domain of subunit II was used (*21*). Excess antibody fragment was removed by HPLC gel filtration (*21*). Site-directed mutagenesis was performed according to ref *16*.

Steady-state measurements of activity with reduced horse heart cytochrome *c* were carried out as described by Witt et al. (*22*) and Pfitzner et al. (*16*). The proton-per-electron ratio of whole cells respiring on succinate was determined according to Puustinen et al. (*23*) and Pfitzner et al. (*16*).

The spectroelectrochemical cell for the Vis and IR range was used as described previously (*24, 25*) with a chemically modified gold grid working electrode (*17*). To accelerate the redox reactions, 16 different mediators were added as described in Hellwig et al. (*17*) to a final concentration of 45 μM each. At this concentration, and with the cell path length below 8 μm, no spectral contributions from the mediators in the VIS and IR range could be detected in control experiments with samples lacking the protein, except for the P═O modes of the phosphate buffer between 1200 and 1000 cm^{-1}.

For electrochemistry, 6 μL of an approximately 0.5 mM cytochrome *c* oxidase solution was diluted in 500 μL of 200 mM phosphate buffer, pH 7.0, containing 100 mM KCl and 3.2 mM *n*-decyl-β-D-maltoside. After 24 h incubation at 4 °C, the sample was concentrated to the initial volume using Microcon ultrafiltration cells (Amicon, Witten, Germany). FTIR and Vis difference spectra as a function of the applied potential were obtained simultaneously by combining an IR (4000−1000 cm^{-1}) and a Vis beam (400−900 nm) as described previously (*26*). For difference spectra, the samples were equilibrated at an initial potential at the electrode, and single-beam spectra in the Vis and the IR range were recorded as references. After equilibrating the samples at the

Table 2: Enzymatic Turnover of Purified Mutant Cytochrome *c* Oxidases from *Paracoccus denitrificans* and Proton-to-Electron Stoichiometries Measured in Intact Cells[a]

P. denitrificans strain	cytochrome *c* oxidase act. (%)	proton pumping (H^+/e^-)
PD1222	100	3.2
AO1	−	2.0
W87Y	87	3.1
W87F	83	3.3
W164F	25	2.7
H403A	59	3.2
Y406F	55	3.3
R473K	93	3.2
R474K	103	3.3

[a] Cytochrome *c* oxidase activities of the mutant enzymes are given relative to the wild-type protein; 100% is equivalent to a turnover number of about 200 s^{-1} at 20 μM cytochrome *c*. The proton-per-electron ratio in succinate-respiring *Paracoccus denitrificans* cells is 3 H^+/e^- in the presence of a redox-driven cytochrome *c* oxidase proton pump and 2 H^+/e^- if the cytochrome bc_1 is bypassed and oxygen is reduced exclusively by quinol oxidase (refs *16* and *23*). As references, proton-per-electron ratios have been determined for the wild-type strain PD1222 and the cytochrome *c* oxidase deficient strain AO1 (ref *16*). The proton-per-electron ratios given were calculated by averaging three measured values, which deviate by a maximum of 0.2 H^+/e^- from each other.

final potential, further single-beam spectra were recorded. Difference spectra as presented in this work were calculated from two single-beam spectra, recorded after complete oxidation and reduction of cytochrome *c* oxidase (at 0.5 and −0.5 V, respectively). The potentials quoted with the data refer to the Ag/AgCl/3 M KCl reference electrode [add +208 mV for SHE′ potentials (pH 7)]. Typically, 128 interferograms at 4 cm^{-1} resolution were co-added for each single-beam spectrum and Fourier-transformed using triangular apodization. To improve the signal-to-noise ratio, 5−10 difference spectra were averaged. Simultaneously recorded UV/Vis difference spectra were used to ensure that repeated reduction−oxidation did not lead to sample deterioration. No smoothing or deconvolution procedures were applied. The noise level was estimated at frequencies above 1780 cm^{-1}, where no signal appears, to be around $(25-50) \times 10^{-6}$ absorbance units and slightly higher in the region of strong absorbance of the sample, such as around 1650 cm^{-1} (water OH modes and amide I modes). Further details of the electrochemical and spectroscopic measurements are described by Hellwig et al. (*17*).

RESULTS AND DISCUSSION

Characterization of the Mutant Cytochrome c Oxidases. The seven mutant enzymes (W87F, W87Y, W164F, H403A, Y406F, R473K, and R474K) were first characterized by measurements of electron-transfer activity and proton pumping (Table 2). The cytochrome *c* oxidase variants W87Y, W87F, R473K, and R474K showed no remarkable decrease of cytochrome *c* oxidase activity in comparison to the wild-type enzyme and no alterations in their optical spectra (not shown). The proton pumping efficiencies were also unchanged (Table 2).

Arginines 473 and 474 are both very highly conserved among the members of the heme/copper oxidase family. Both residues, as well as the heme propionates, are part of a cluster of ionizable groups electrostatically interacting with each other and with the cofactors (*27*). Upon reduction of the binuclear center, one proton is calculated to be accepted by this cluster (*27*). Recently, in the related quinol oxidase from *E. coli*, R481 and R482 (R473 and R474 in *P. denitrificans*) have been exchanged to glutamine, asparagine, and leucine (*28*). For the mutant enzymes R482N, R482L, R482Q, and R481Q, decreased enzymatic activity has been found, whereas the proton pumping stoichiometry remained unchanged. In contrast, in the mutant enzymes R481N and R481L and the double mutant enzyme R481Q/R482Q, significant residual enzymatic activity but a loss of proton pumping was detected (*28*). From these results and from electrostatic calculations (*27*), it has been argued that the arginine residues might stabilize the deprotonated forms of the ring D propionates, especially the ring D propionate of heme a_3, which is supposed to function as proton acceptor in a crucial step of the proton translocation mechanism (*28*). In the present study, the lysine residues introduced at positions R473 and R474 in cytochrome *c* oxidase from *Paracoccus denitrificans* completely fulfilled the role of the arginine residues concerning enzymatic turnover and proton pumping.

The cytochrome *c* oxidase variants H403A and Y406F showed significantly lower cytochrome *c* oxidase activities than the wild-type enzyme, whereas the proton pumping activities of these two mutants were equivalent to that of the wild-type. These results agree with the published data of the corresponding cytochrome *c* oxidase variants H411A and Y414F from *Rhodobacter sphaeroides* (*29*). The cytochrome *c* oxidase activities of these mutant enzymes, measured with purified proteins, were 41% and 47% of the wild-type activity, respectively. The proton pumping efficiencies, however, were not affected. The Vis spectrum of Y414F showed a 5 nm red shift of the α-band whereas the spectrum of H411A showed a 0.8 nm blue shift of the α-band (*29, 30*). In reduced-minus-oxidized Vis difference spectra of the *P. denitrificans* enzyme variant H403A, no significant alteration could be identified, whereas for the variant Y406F a 5 nm red shift of the α-band has been observed (Figure 2) as in the corresponding *Rhodobacter sphaeroides* mutant enzyme. The separation of the spectral contributions of heme *a* and heme a_3 (*31*) revealed red shifts of 5 nm for both α-bands (not shown). Due to the close vicinity of Y406 to heme *a*, mutation of this residue is very likely to affect the absorption of heme *a*. In contrast, it was not expected that this mutation would also affect the absorption of heme a_3.

In the W164F variant, the enzymatic activity was reduced more drastically, which might also account for the decrease of the proton-per-electron ratio. In *P. denitrificans* cells, electron transfer from succinate to oxygen via the succinate dehydrogenase, cytochrome bc_1, and cytochrome *c* oxidase results in acidification of the external medium with a stoichiometry of 3 protons per electron. In mutant W164F, a significant amount of the produced quinol could be oxidized by the quinol oxidase instead of cytochrome bc_1, thus causing the slightly reduced value for the proton-per-electron ratio.

Reduced-Minus-Oxidized FTIR Difference Spectra of Mutant Enzymes. As shown in Figure 1 and Table 1, the ring A propionate of heme *a* is within hydrogen bonding distance to Y406 and W87. For the assignment of the signals in the reduced-minus-oxidized FTIR difference spectrum to specific heme propionates, the Y406F variant seems to be

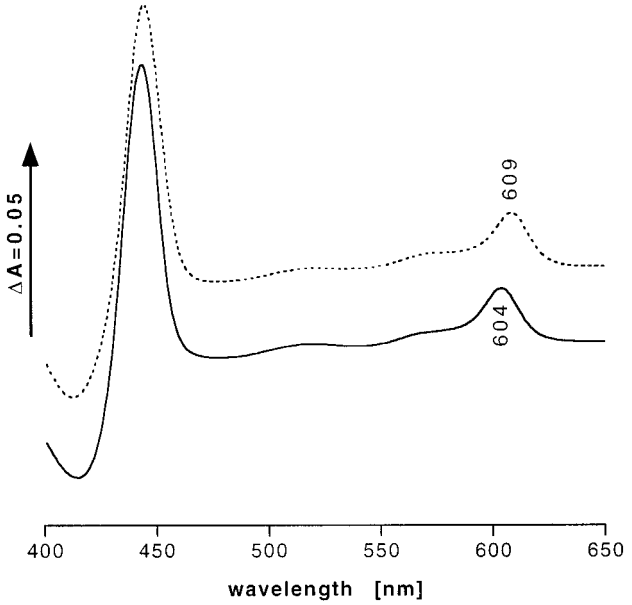

FIGURE 2: Electrochemically induced reduced-minus-oxidized optical spectra of purified wild-type cytochrome *c* oxidase (solid line) and mutant enzyme Y406F (dashed line).

unfavorable because of the obvious perturbance of the heme groups. The mutant enzymes W87F and W87Y, however, were suitable for that purpose, and the corresponding reduced-minus-oxidized FTIR difference spectra were almost identical. The reduced-minus-oxidized FTIR difference spectrum of the W87F variant is presented in Figure 3, together with the spectrum of the wild-type enzyme, which has been published and extensively discussed in Hellwig et al. (*31*, *32*).

In the W87F variant, no hydrogen bond to the ring A propionate of heme *a* can be formed; thus, the vibrational modes of this propionate are assumed to be altered after mutation. When the spectra of the mutant and the wild-type enzyme were compared, only small differences could be detected. Besides minor variations in the region of strong absorbance of the sample (at 1642 and 1660 cm^{-1}), the amplitude of the positive signal at 1546 cm^{-1} was slightly reduced. This is shown in expanded scale in Figure 4 A together with a double difference spectrum in Figure 4B. This signal is located within the range where a positive signal has been assigned to an antisymmetric COO^- mode of a deprotonated heme propionate, which appears upon reduction of the cytochrome *c* oxidase (*15*). Neither vibrational modes of a tryptophan nor those of a phenylalanine are expected in this spectral region (*33*, *34*).

The ring D propionate of heme *a* is within hydrogen bonding distance of the backbone NH group of W164, of the ϵNH group and one NH_2 group of R474, of one NH_2 group of R473, and of a water molecule (Table 1). The ring D propionate of heme a_3 is in hydrogen bonding distance of the ring NH group of W164, of both terminal N atoms of R473, and of another water molecule (Table 1). In the cytochrome *c* oxidase variant W164F, enzymatic turnover was significantly decreased, indicating structural changes within the protein. This was confirmed by the reduced-minus-oxidized FTIR difference spectrum (not shown), which differs considerably from that of the wild-type enzyme, It is thus not included for the analysis of the propionate group interaction discussed here.

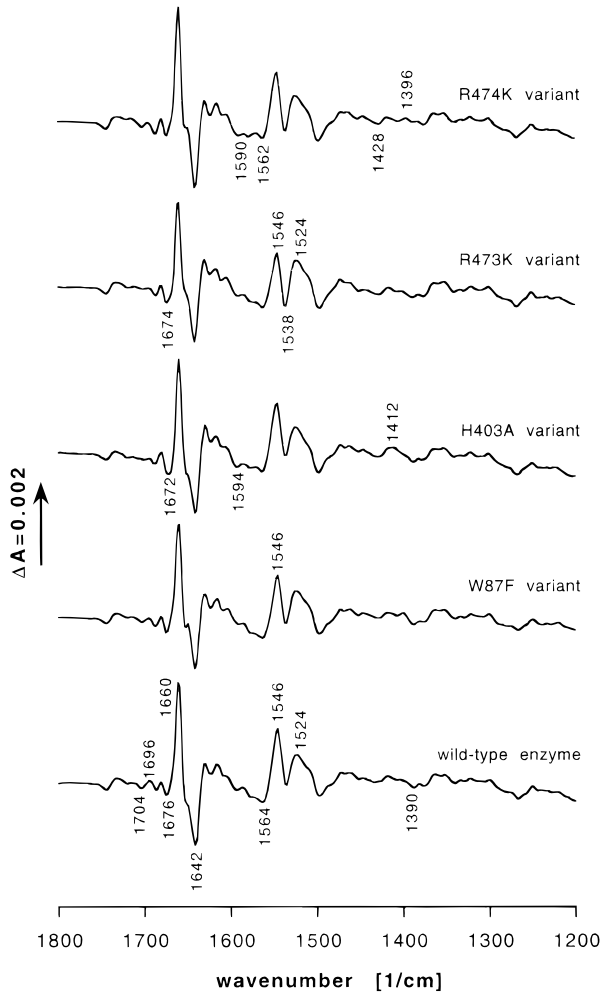

FIGURE 3: Reduced-minus-oxidized FTIR difference spectra of the wild-type enzyme and the mutant enzymes W87F, H403A, R473K, and R474K obtained for a potential step from 0.5 to −0.5 V (vs Ag/AgCl/3 M KCl). Conditions: approximately 0.5 mM cytochrome *c* oxidase in 200 mM phosphate buffer, pH 7, with 100 mM KCl as electrolyte and mediators as described under Experimental Procedures.

The reduced-minus-oxidized FTIR difference spectra of the enzyme variants R474K and R473K are presented in Figure 3. The spectrum of R474K differed only in two regions from the spectrum of the wild-type enzyme: between 1590 and 1560 cm^{-1}, and between 1430 and 1390 cm^{-1}. These regions are shown expanded together with the spectrum of the wild-type enzyme in Figures 5A and 6A, and as double difference spectra in Figures 5B and 6B, respectively. Neither bands from arginine nor bands from lysine side chains are expected in these spectral regions (*35*). In a previous study, a negative band at 1570 cm^{-1} has clearly been assigned to an antisymmetric COO^- mode of a heme propionate by isotopic labeling (*15*). It is this signal which is shifted to higher wavenumbers (1588 cm^{-1}) in the spectrum of the mutant enzyme (Figure 5). The negative band at 1388 cm^{-1}, recently assigned to a symmetric COO^- mode of a heme propionate (*15*), has been additionally shifted to higher wavenumbers (1430−1400 cm^{-1}) in the spectrum of the R474K variant (Figure 6).

In the spectrum of the cytochrome *c* oxidase variant R473K, significant changes occurred in the 1546−1538 cm^{-1} range, as shown expanded in Figure 7. Positive contributions, partially assigned to a heme propionate COO^- mode (*15*),

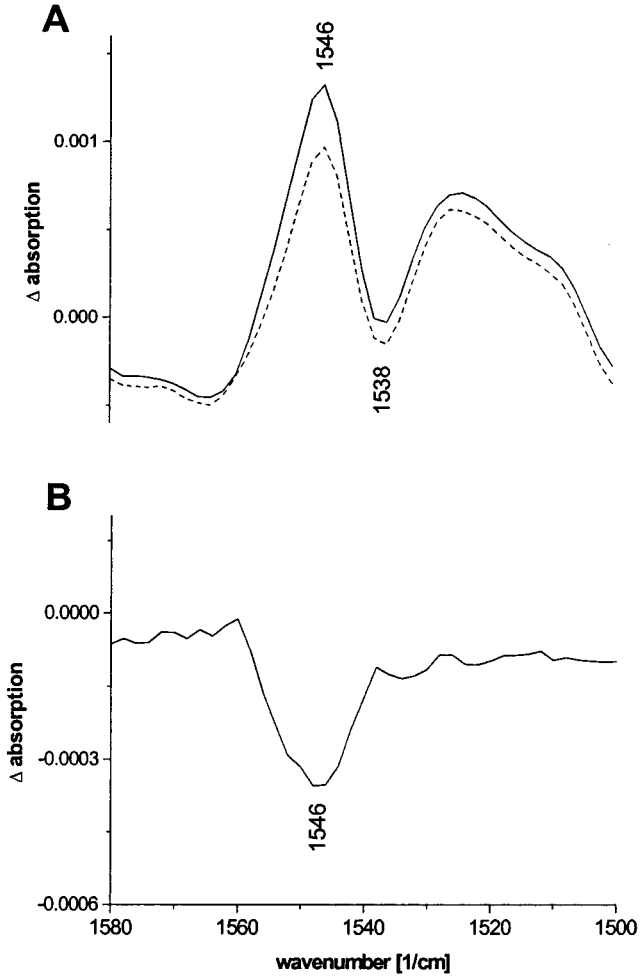

FIGURE 4: The 1565−1525 cm^{-1} region of the reduced-minus-oxidized FTIR difference spectra of the wild-type enzyme (solid line) and the mutant enzyme W87F (dashed line) obtained for a potential step from 0.5 to −0.5 V (A) and the double difference spectrum obtained by subtracting the spectrum of the W87F mutant enzyme from wild-type enzyme (B). Conditions as described in Figure 3.

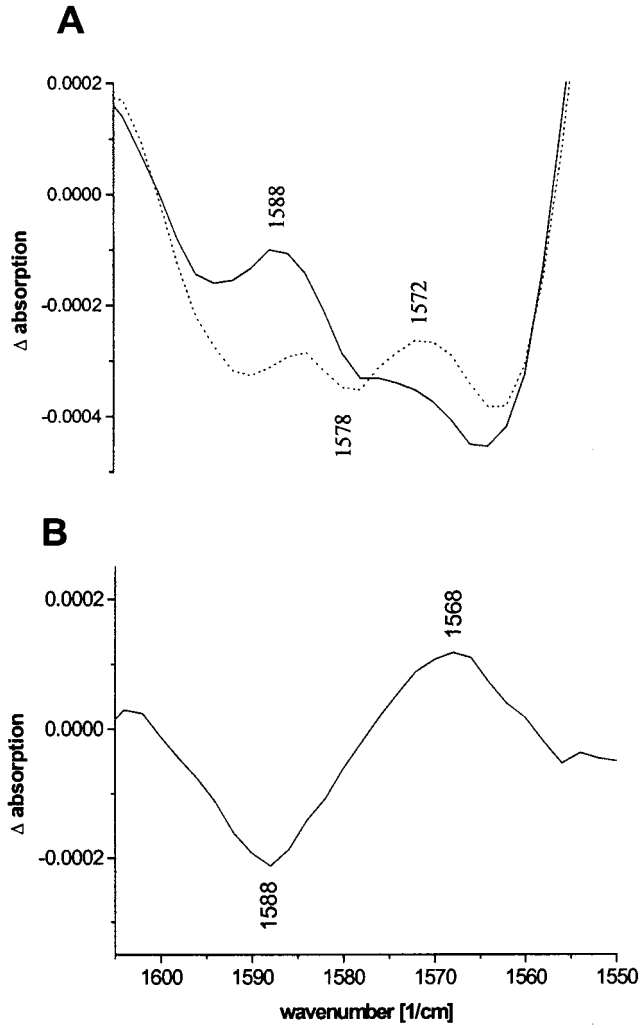

FIGURE 5: The 1605−1550 cm^{-1} region of the reduced-minus-oxidized FTIR difference spectra of the wild-type enzyme (solid line) and the mutant enzyme R474K (dashed line) obtained for a potential step from 0.5 to −0.5 V (A) and the double difference spectrum obtained by subtracting the spectrum of the R474K mutant enzyme from wild-type enzyme (B). Conditions as described in Figure 3.

are decreased in this spectral region. Very small spectral alterations have been also observed at 1704 and 1696 cm^{-1}, where a positive and a negative signal decreased slightly in amplitude (see Figure 3). The band at 1676 cm^{-1} has been shifted to 1674 cm^{-1}, probably because of the disappearance of a positive contribution of the R473 $\nu_{as}(CN_3H_5^+)$ mode, which is expected in this spectral range (*32*, *35*).

The ring A propionate of heme a_3 is in hydrogen bonding distance to H403, to D399, and to a water molecule. The electrochemically induced FTIR difference spectrum of cytochrome *c* oxidase variant D399N has been published in Hellwig et al. (*17*). In addition to the negative band at 1676 cm^{-1}, a composed band which was assigned partially to a COOH mode of a protonated heme propionate, a negative signal at 1672 cm^{-1} appeared, which might be caused by the introduced asparagine residue absorbing in this spectral range (Hellwig et al., unpublished results). In the spectrum of the H403A variant, a similar change occurred (Figure 8). This result might be due to a modification of the heme propionate COOH mode or changes of the formyl group vibration of heme a_3 (*32*). We keep in mind, that additionally, changes of amide I modes are possible in this spectral range (*32*). These effects might lead to the spectral changes in the spectrum of the D399N variant in addition to those arising from the asparagine absorption. In both spectra, that of the D399N variant and that of the H403A variant, a positive signal at 1412 cm^{-1} appears (cf. Figure 3). This signal may reflect a shifted and intensity-changed $\nu(COO^-)$ mode. A clear attribution, however, is not clear yet on the basis of the spectra available. The spectral change at 1594 cm^{-1} in the reduced-minus-oxidized FTIR difference spectra of the mutant enzyme H403A is probably due to the absence of the $\nu(C{=}C)$ mode of H403. An assignment of this mode finds some support from Raman spectra of polypeptides containing L-histidine residues (*36*). On the other hand, the infrared absorption of the His $\nu(C{=}C)$ mode is very weak (*35*), leaving open a conclusive assignment. Beside the changes mentioned, the spectra of both cytochrome *c* oxidase variants H403A and D399N were close to that of the wild-type enzyme. Some very small variations appear that may be induced by very minor structural changes upon mutation.

Band Assignment to Specific Heme Propionates. The negative signal at 1676 cm^{-1} in the spectrum of the wild-type enzyme might partially be attributed to the ring A

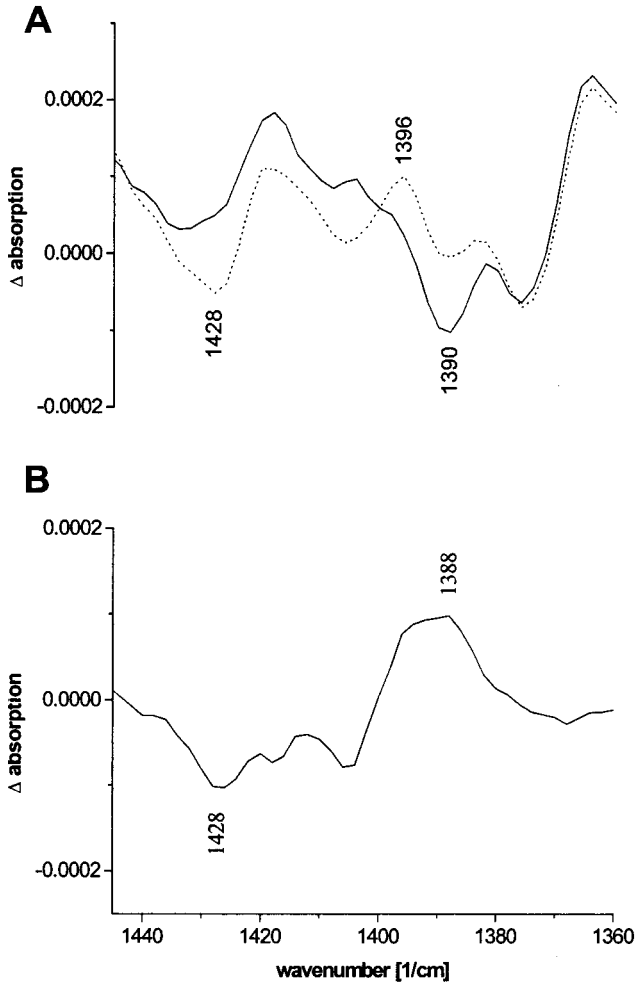

FIGURE 6: The 1450−1360 cm^{-1} region of the reduced-minus-oxidized FTIR difference spectra of the wild-type enzyme (solid line) and the mutant enzyme R474K (dashed line) obtained for a potential step from 0.5 to −0.5 V (A) and the double difference spectrum obtained by subtracting the spectrum of the R474K mutant enzyme from wild-type enzyme (B). Conditions as described in Figure 3.

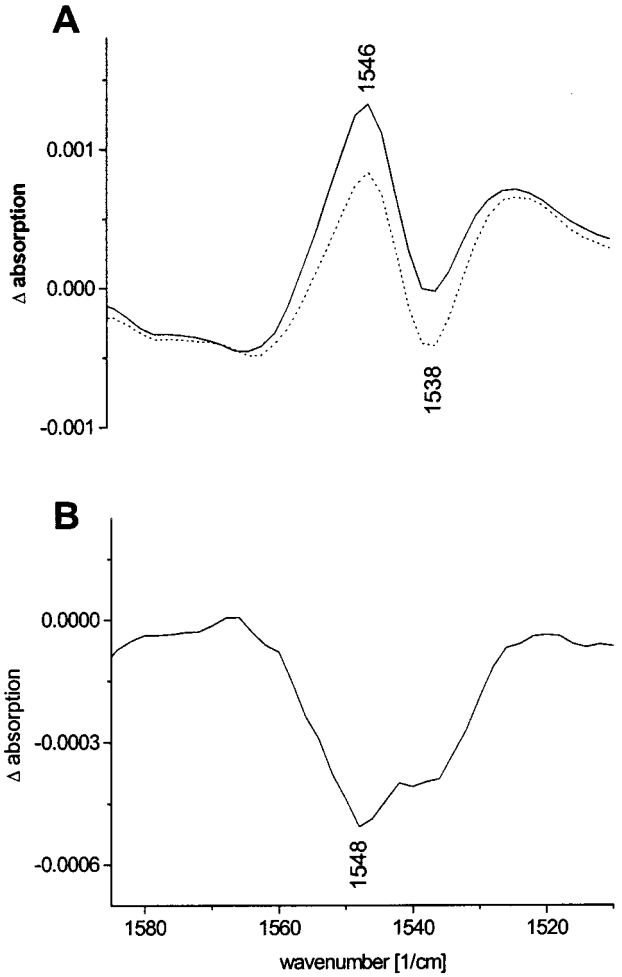

FIGURE 7: The 1570−1520 cm^{-1} region of the reduced-minus-oxidized FTIR difference spectra of the wild-type enzyme (solid line) and the mutant enzyme R473K (dashed line) obtained for a potential step from 0.5 to −0.5 V (A) and the double difference spectrum obtained by subtracting the spectrum of the R473K mutant enzyme from wild-type enzyme (B). Conditions as described in Figure 3.

propionate of heme a_3, as indicated by the spectrum of the H403A variant. This heme propionate is proposed to undergo environmental changes upon reduction of cytochrome *c* oxidase. In the case of protonation/deprotonation of this heme propionate, spectral alterations would also be expected in the range of the antisymmetric COO^- modes of the heme propionates. A shift was observed at 1594 cm^{-1}, however, tentatively attributed to a histidine mode, as described above. Neither at 1570 cm^{-1} nor in the region 1546−1528 cm^{-1} have changes been observed in the spectrum of the H403A variant, and thus a protonation/deprotonation of this heme propionate can be excluded. Nevertheless, the assignment to the ring A propionate of heme a_3 is not that clear, because, as mentioned, the changes of the signal at 1676 cm^{-1} might also be associated with alterations of the formyl group mode of heme a_3 or changes of amide I modes (*32*).

A major part of the positive signal at 1546−1528 cm^{-1}, previously assigned to a heme propionate mode, can be attributed to the ring D propionate of heme a_3. Whereas the positive signal in the spectrum of the R473K variant decreased, it was completely unchanged in the spectrum of the R474K variant, indicating that the ring D propionate of heme *a* was not affected by the change of R473 to lysine.

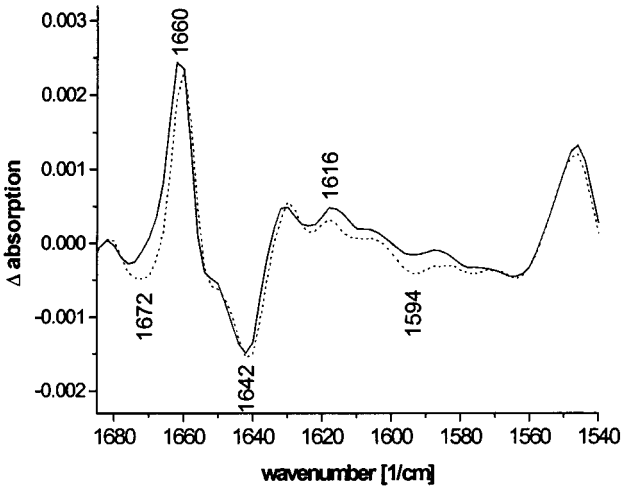

FIGURE 8: The 1685−1540 cm^{-1} region of the reduced-minus-oxidized FTIR difference spectra of the wild-type enzyme (solid line) and the mutant enzyme H403A (dashed line) obtained for a potential step from 0.5 to −0.5 V. Conditions as described in Figure 3.

However, this mutation obviously resulted in a p*K* shift or an environmental change of the ring D propionate of heme

a_3. The correlation of the signal at 1528 cm^{-1} with heme a_3 electron transfer was shown previously (*32*).

This assignment either suggests a deprotonation of the ring D propionate of heme a_3 upon reduction of cytochrome *c* oxidase, or more probably points to conformational changes. The former is unlikely, because the electrostatic calculation (*27*) indicates that this propionate is deprotonated in the oxidized state of cytochrome *c* oxidase. The latter would imply that mainly the extinction coefficient of the COO^- mode changed upon reduction of the protein whereas the vibrational frequency remained almost unchanged.

A minor part of the 1546−1528 cm^{-1} signal might also be due to a COO^- mode of the ring A propionate of heme *a*, because in the spectra of cytochrome *c* oxidase variants W87F and W87Y the intensity of the positive signals at 1546 cm^{-1} was slightly reduced. Since the changes observed are very small, this assignment has to be considered less reliable, until further data are available.

As a result of the spectral characterization of the R474K variant, both the negative signal at 1570 cm^{-1} and the negative signal at 1390 cm^{-1} (assigned to an antisymmetric and a symmetric COO^- mode of a heme propionate, respectively) can be attributed to the ring D propionate of heme *a*. As already mentioned, the ϵNH group and one of the NH_2 groups of R474 are in hydrogen bonding distance to the ring D propionate of heme *a*. In addition, the backbone NH group is in hydrogen bonding distance to the ring A propionate of heme *a*, and R474 interacts electrostatically with the ring D propionate of heme a_3. Neither the mutant enzymes W87F and W87Y nor the R473K variant showed alterations in these spectral regions. Thus, the assignment of the two signals to the ring D propionate of heme *a* seems to be unequivocal. The shift of the signal at 1570 cm^{-1} to 1590 cm^{-1} in the spectrum of the R474K variant indicates a stronger stabilization of the deprotonated heme propionate as a result of the mutation (*37*, *38*). With this argumentation, the symmetric COO^- mode is predicted to shift to lower wavenumbers (*37*, *38*). In contrast, the band at 1390 cm^{-1} has been shifted to higher wavenumbers in the spectrum of the R474K variant. The introduced lysine residue not only changed the p*K* value of the heme propionate but also changed the heme propionate environment, so that the direction of the shift is not predictable.

The assignment of both signals, the symmetric and the antisymmetric mode, to the ring D propionate of heme *a* indicates that the propionate is protonated upon reduction of cytochrome *c* oxidase, or, less likely, undergoes environmental changes. In the latter case, mainly the extinction coefficients of the antisymmetric and the symmetric COO^- modes were affected, in contrast to the vibrational frequencies. This scenario seems to be improbable, although it cannot be ruled out completely. In the case of a protonation reaction, the ν(C═O) mode of the COOH group might appear in the region of strong absorption of the sample below 1675 cm^{-1}. This spectral range is highly overlapped with bands from the amide I absorption; it is difficult to detect here.

CONCLUSIONS

The ring D propionate of heme *a* probably acts as a proton acceptor upon reduction of cytochrome *c* oxidase. As revealed by this study, none of the other three heme propionates seems to be protonated upon reduction of the enzyme. The ring D propionate of heme a_3 might undergo significant conformational changes in its charged state, which might result in a change of the proton arrangement within the cluster of interacting residues and thus cause an increase in net protonation. This would be in line with the prediction by Kannt et al. (*27*). As a consequence, disturbance of this cluster by the mutations R473N, R473L, and R473Q/R474Q (*P. denitrificans* numbering) is expected to result in a loss of proton pumping activity as observed in the quinol oxidase from *E. coli* (*28*).

ACKNOWLEDGMENT

We thank Bernd Ludwig (Frankfurt) for providing the mutagenesis system, and along with his co-workers Oliver-Matthias H. Richter and Ute Pfitzner for supporting the proton pumping experiments. We are further grateful to Axel Harrenga for structural data and Hannelore Müller and Christine Ernd for excellent technical assistance.

REFERENCES

1. Iwata, S., Ostermeier, C., Ludwig, B., and Michel, H. (1995) *Nature 376*, 660−669.
2. Ostermeier, C., Iwata, S., Ludwig, B., and Michel, H. (1995) *Nat. Struct. Biol. 2*, 842−846.
3. Thomas, J. W., Puustinen, A., Alben, J. O., Gennis, R. B., and Wikström, M. (1993) *Biochemistry 32*, 10923−10928.
4. García-Horsman, J. A., Puustinen, A., Gennis, R. B., and Wikström, M. (1995) *Biochemistry 34*, 4428−4433.
5. Yoshikawa, S., Shinzawa-Itoh, K., Nakashima, R., Yaono, R., Yamashita, E., Inoue, N., Yao, M., Fei, M. J., Libeu, C. P., Mizushima, T., Yamaguchi, H., Tomizaki, T., and Tsukihara, T. (1998) *Science 280*, 1723−1729.
6. Hosler, J. P., Shapleigh, J. P., Mitchell, D. M., Kim, Y., Pressler, M. A., Georgiou, C., Babcock, G. T., Alben, J. O., Ferguson-Miller, S., and Gennis, R. B. (1996) *Biochemistry 35*, 10776−10783.
7. Mills, D. A., and Ferguson-Miller, S. (1998) *Biochim. Biophys. Acta 1365*, 46−52.
8. Wikström, M. (1989) *Nature 338*, 776−778.
9. Michel, H. (1998) *Proc. Natl. Acad. Sci. U.S.A. 95*, 12819−12824.
10. Vygodina, T. V., Pecoraro, C., Mitchell, D., Gennis, R., and Konstantinov, A. A. (1998) *Biochemistry 37*, 3053−3061.
11. Kannt, A., Lancaster, C. R. D., and Michel, H. (1998) *Biophys. J. 74*, 708−721.
12. Mitchell, R., and Rich, P. R. (1994) *Biochim. Biophys. Acta 1186*, 19−26.
13. Capitanio, N., Vygodina, T. V., Capitanio, C., Konstantinov, A. A., Nicholls, P., and Papa, S. (1997) *Biochim. Biophys. Acta 1318*, 255−265.
14. Rich, P. R. (1995) *Aust. J. Plant Physiol. 22*, 479−486.
15. Behr, J., Hellwig, P., Mäntele, W., and Michel, H. (1998) *Biochemistry 37*, 7400−7406.
16. Pfitzner, U., Odenwald, A., Ostermann, T., Weingard, L., Ludwig, B., and Richter, O.-M. H. (1998) *J. Bioenerg. Biomembr. 30*, 89−97.
17. Hellwig, P., Behr, J., Ostermeier, C., Richter, O. M. H., Pfitzner, U., Odenwald, A., Ludwig, B., Michel, H., and Mäntele, W. (1998) *Biochemistry 37*, 7390−7399.
18. Ludwig, B. (1986) *Methods Enzymol. 126*, 153−159.
19. Gerhus, E., Steinrücke, P., and Ludwig, B. (1990) *J. Bacteriol. 172*, 2393−2400.
20. Kleymann, G., Ostermeier, C., Ludwig, B., Skerra, A., and Michel, H. (1995) *Bio/Technology 13*, 155−160.
21. Ostermeier, C., Harrenga, A., Ermler, U., and Michel, H. (1997) *Proc. Natl. Acad. Sci. U.S.A. 94*, 10547−10553.
22. Witt, H., and Ludwig, B. (1997) *J. Biol. Chem. 272*, 5514−5517.

23. Puustinen, A., and Wikström, M. (1999) *Proc. Natl. Acad. Sci. U.S.A. 96*, 35−37.
24. Moss, D. A., Nabedryk, E., Breton, J., and Mäntele, W. (1990) *Eur. J. Biochem. 187*, 565−572.
25. Mäntele, W. (1996) in *Biophysical Techniques in Photosynthesis* (Hoff, A. J., and Amesz, J., Eds.) Chapter 9, pp 137−160, Kluwer, Dordrecht.
26. Mäntele, W. (1993) *Trends Biochem. Sci. 18*, 197−202.
27. Karpefors, M., Ädelroth, P., Aagaard, A., Sigurdson, H., Ek, M. S., and Brzezinski, P. (1998*) Biochim. Biophys. Acta 1365*, 159−169.
28. Puustinen, A., Finel, M., Virkki, M., and Wikström, M. (1989) *FEBS Lett. 249*, 163−167.
29. Fetter, J. R., Qian, J., Sphapleigh, J., Thomas, J. W., García-Horsman, A., Schmidt, E., Hosler, J., Babcock, G. T., Gennis, R. B., and Ferguson-Miller, S. (1995) *Proc. Natl. Acad. Sci. U.S.A. 92*, 1604−1608.
30. Hosler, J. P., Espe, M. P., Zhen, Y., Babcock, G. T., and Ferguson-Miller, S. (1995) *Biochemistry 34*, 7586−7592.
31. Hellwig, P., Rost, B., Kaiser, U., Ostermeier, C., Michel, H., and Mäntele, W. (1996) *FEBS Lett. 385*, 53−57.
32. Hellwig, P., Grzybek, S., Behr, J., Ludwig, B., Michel, H., and Mäntele, W. (1999) *Biochemistry 38*, 1685−1694.
33. Lautié, A., Lautié, M. F., Gruger, A., and Fakhri, S. A. (1980) *Spectrochim. Acta 36A*, 85−94.
34. Takeuchi, H., and Harada, I. (1986) *Spectrochim. Acta 42A*, 1069−1078.
35. Venyaminov, S. Y., and Kalnin, N. N. (1990) *Biopolymers 30*, 1259−1271.
36. Ashikawa, I., and Itoh, K. (1979) *Biopolymers 18*, 1859−1876.
37. Koeppe, R. E., and Stroud, R. M. (1976) *Biochemistry 15*, 3450−3458.
38. Wright, W. W., Laberge, M., and Vanderkooi, J. M. (1997) *Biochemistry 36*, 14724−14732.

BI991504G